CHIN. PHYS. LETT. Vol. 36, No. 7 (2019) 074202

Generation of Gaussian-Shape Single Photons for High Efficiency Quantum Storage *

Jian-Feng Li(李建锋)[1], Yun-Fei Wang(王云飞)[1], Ke-Yu Su(苏柯宇)[1], Kai-Yu Liao(廖开宇)[1], Shan-Chao Zhang(张善超)[1], Hui Yan(颜辉)[1**], Shi-Liang Zhu(朱诗亮)[2,1**]

[1]*Guangdong Provincial Key Laboratory of Quantum Engineering and Quantum Materials, GPETR Center for Quantum Precision Measurement and SPTE, South China Normal University, Guangzhou 510006*

[2]*National Laboratory of Solid State Microstructures, School of Physics, Nanjing University, Nanjing 210093*

(Received 11 March 2019)

We report the generation of heralded single photons with Gaussian-shape temporal waveforms through the spatial light modulation technique in an atomic ensemble. Both the full width at half maximum and the peak position of the Gaussian waveform can be controlled while the single photon nature holds well. We also analyze the bandwidth of the generated single photons in frequency domain and show how the sidebands of the frequency spectrum are modified by the shape of the temporal waveform. The generated single photons are especially suited for the realization of high efficiency quantum storage based on electromagnetically induced transparency.

PACS: 42.50.−p, 32.80.−t, 03.67.−a DOI: 10.1088/0256-307X/36/7/074202

A highly controllable paired photon source is of great interest, not only for its application in the fundamental research,[1−3] but also for its essential role in quantum information processing.[4−7] In the past several decades, photon pairs are usually produced from spontaneous parametric down-conversion process, which have a wide bandwidth (>THz).[8−10] Heralded single photons with such a wide bandwidth are hard to realize strong enough interaction with atoms, which is required for memory-based quantum networks.[11−17] Later, a new type of single photon source based on the electromagnetically induced transparency (EIT)-assisted spontaneous four-wave mixing (SFWM), which generates pair photons in an atomic ensemble, was reported.[18−30] With the help of the EIT slow light effect, heralded photons with long coherent times were generated and a subnatural line width was achieved. However, to store and couple the single photons with atoms or cavity efficiently, having only a narrow bandwidth in the frequency domain is not enough. The optimization of the temporal waveform is also required.[31−33] Although an arbitrary temporal waveform can be realized using an electro-optic modulator (EOM),[34] an unavoidable loss will be introduced. Another method that shapes the heralded single photon's waveform with modulated classical fields has also been realized,[35] which also limits its application because of its low generating rate. Recently, a more practical idea has been demonstrated to shape the temporal waveform by the spatial-light-modulation technique.[36,37] This method greatly simplifies the process and simultaneously reduces the loss.

As for the realization of high efficiency quantum storage through EIT, single photons with Gaussian-shape temporal waveform are preferred.[15,16] The spatial-light-modulation technique is a good choice for generating such a waveform. This method can still be improved in practical applications. In this Letter, we report the generation of Gaussian-shape heralded single photons with a simpler spatial-light-modulation method. Instead of using a spatial-light modulator (SLM), we use an aspheric lens to shape the pump beam and then control the single photon's waveform. Compared with the SLM setup which potentially has active electronic noise, this lens-based method is more reliable.

The energy level configuration of the SFWM is shown in Fig. 1(c). The frequency of the pump beam ($\omega_{\rm p}$) is off resonance and the frequency of the coupling beam ($\omega_{\rm c}$) is on resonance. In the presence of these two beams, a pair of a Stokes photon ($\omega_{\rm s}$) and anti-Stokes photon ($\omega_{\rm as}$) are generated from the atomic ensemble through the SFWM process. The pump beam is far detuning and its Rabi frequency is extremely small to suppress the multi-photon generation probability to guarantee the single photon nature of the source. The experimental setup is shown in Fig. 1(a), and a cigar-shaped two-dimensional (2D) magneto-optical trap (MOT) is used to generate the heralded single photons. The longitudinal length of the atomic ensemble is $L = 1.7$ cm and the optical depth (OD) of the MOT is optimized to about 120 by applying the dark-line MOT technique.[38−40] In the presence of the counter-propagating pump beam (780 nm, σ^-, $\omega_{\rm p}$)

*Supported by the National Key Research and Development Program of China under Grant Nos 2016YFA0301800 and 2016YFA0302800, the National Natural Science Foundation of China under Grant Nos 11822403, 91636218, U1801661, 11704131, 11804105 and 11804104, the Natural Science Foundation of Guangdong Province under Grant Nos 2015TQ01X715 and 2018A0303130066, and the KPST of Guangzhou under Grant No 201804020055.

**Corresponding author. Email: yanhui@scnu.edu.cn; slzhu@nju.edu.cn

© 2019 Chinese Physical Society and IOP Publishing Ltd

and coupling beam (795 nm, σ^+, ω_c), a pair of phase-matched counter-propagating Stokes (780 nm, σ^-, ω_s) and anti-Stokes (795 nm, σ^+, ω_{as}) photons will be produced along the longitudinal direction of the atomic ensemble. Here the angle between the Stokes/anti-Stokes axis (z axis) and the pump/coupling (z' axis) is chosen to be $\theta = 3.14°$ to provide spatial separation of the weak Stokes and anti-Stokes fields from the strong pump and coupling fields, while also helping to generate the profile of the pump beam on the z axis simultaneously as shown in Fig. 1(b). Both the coupling beam and the pump beam are Gaussian beams. The coupling beam is collimated and the beam diameter ($1/e^2$) is about 1.8 mm. The pump beam has a frequency blue detune of 80 MHz from the transition $|1\rangle \leftrightarrow |4\rangle$ and is focused onto the MOT by an aspheric lens (THORLABS, A375TM-B) of 7.5 mm focal length and the waist radius is 450 μm. The distance from the lens to the atomic ensemble is about 133 cm. Between the lens and the atomic ensemble, a high-reflectivity mirror mounted on a linear translation stage (LTS) is used and the pump beam is incident on the mirror with an angle of 45°. By moving the LTS, one can translate the pump beam to shift the spatial profile of the pump beam along the z direction. The generated paired photons are collected by two fiber couplers (FCs). Each fiber coupler contains an aspheric lens (THORLABS, C220TMD-B) and links to a polarization maintaining single mode fiber with numerical aperture of 0.11. The quarter wave plates and the polarizing beam splitters before the FCs are used to convert the circular polarization to the linear polarization for the coupling of the single mode fibers, and also to provide a polarization filtering at the same time. After two narrowband Fabry–Pérot (FP) filters (F_1 and F_2) with isolation ratio of 41 dB, the Stokes and anti-Stokes photons are detected by the single-photon counter modules (SPCMs, Perkin Elmer, SPCM-AQRH-16FC) with dark count rate of 25 counts per second. The detected signals are sent to a fast commercially multiple-event time digitizer (FAST ComTec, P7888) for coincidence measurement.

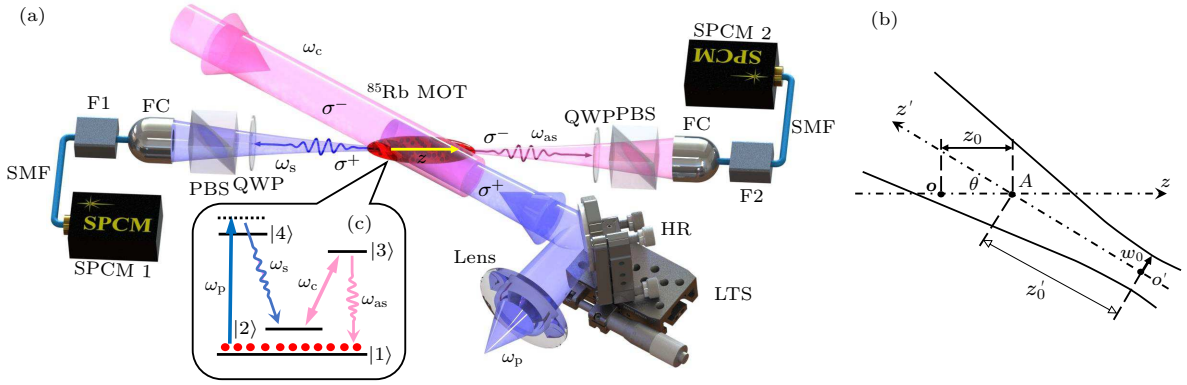

Fig. 1. (a) The experimental setup of the heralded single photon source. MOT: magneto-optical trap; ω_c: coupling beam; ω_p: pump beam; ω_{as}: anti-Stokes photon; ω_s: Stokes photon; QWP: quarter wave plate; PBS: polarizing beam splitter; FC: fiber coupler; F1 and F2: multi-level Fabry–Pérot filter; SMF: single mode fiber; SPCM1 and SPCM2: single-photon counter module; HR: high-reflectivity mirror; LTS: linear translation stage. (b) A simplified model of the pump beam profile along the z direction. O: center of the MOT; O′: waist position of the pump beam; z': optical axis of the pump beam; A: intersection point of the z and z' axis; w_0: waist radius of the pump beam; θ: the angle between z and z' axes. (c) The energy levels for the spontaneous-four-wave-mixing (SFWM) configuration: $|1\rangle = |5S_{1/2}, F = 2\rangle$, $|2\rangle = |5S_{1/2}, F = 3\rangle$, $|3\rangle = |5P_{1/2}, F = 3\rangle$, and $|4\rangle = |5P_{3/2}, F = 3\rangle$.

When the coupling beam is uniform along the z axis and the pump beam has a profile $f_p(z)$ (here $z = 0$ indicates the center of the MOT), the temporal wave function of the heralded single photons can be expressed as[36,37]

$$\psi(\tau) \approx \kappa_0 V_g f_p(L/2 - V_g\tau), \tag{1}$$

where κ_0 is the nonlinear coupling strength of the SFWM process, and $V_g = \Omega_c^2 L/(2\mathrm{OD}\gamma_{13})$ is the group velocity of the heralded single photons (here Ω_c is the Rabi frequency of the coupling beam, and γ_{13} is the decay rate between $|1\rangle$ and $|3\rangle$).

For a simplified model sketched in Fig. 1(b), the profile of the pump beam along the z axis can be described as

$$f_p(z) = \frac{w_0}{w[z_0' - (z - z_0)\cdot\cos\theta]} \cdot e^{-\frac{(z-z_0)^2\cdot\sin^2\theta}{w[z_0'-(z-z_0)\cdot\cos\theta]^2}}, \tag{2}$$

where w_0 is the waist radius of the pump beam, $w(z') = w_0\sqrt{1 + (z'/f)^2}$ is the radius at which the field intensity falls to $1/e^2$ of their axial values at the plane z' along the pump beam, and $f = \pi w_0^2/\lambda$ is the Rayleigh length of the pump beam (λ is the wavelength of the pump beam). As shown in Fig. 1(a), when the LTS has a translation along the z' axis, it will lead to a translation of the pump beam in both z' direction and z direction. If the LTS translates for a length of $\Delta z'$ in z' direction, z_0' will gain a variation

of $-\Delta z'$ while z_0 will gain a variation of $-\Delta z'/\sin\theta$.

In our experiment, as the waist radius of the pump beam is 450 μm, which corresponds to a Rayleigh length of about 80 cm. This is much larger than the scale of the MOT ($z' \ll f$), we could have the approximation of $w[z'_0 - (z - z_0)\cdot\cos\theta] \approx w_0$ and obtain

$$f_{\rm p}(L/2 - V_{\rm g}\tau) = \exp\Big[-\frac{(\tau - \frac{L/2-z_0}{V_{\rm g}})^2\cdot(V_{\rm g}\sin\theta)^2}{w_0^2}\Big]. \quad (3)$$

Equation (3) shows that the FWHM of the heralded single photon's wave function can be controlled by the group velocity of the heralded single photon, which can be modified by changing the Rabi frequency of the coupling beam. The peak position of the heralded single photon's wave function can be controlled by shifting z_0 with the LTS.

First of all, we demonstrate a method to shift the peak position of the heralded single photon's waveform. The Rabi frequency of the coupling beam is set to $\Omega_{\rm c} = 2\pi\times 13.0$ MHz. The Rabi frequency of the pump beam at the beam waist is set to $\Omega_{\rm p} = 2\pi\times 1.6$ MHz. Then we adjust the LTS to obtain different profiles of the pump beam on the z axis, as shown in Figs. 2(a1)–2(a3). The main results are shown in Figs. 2(a2), 2(b2) and 2(c2). Here the theoretical curve is calculated from the theory in Ref. [37]. The measurement time for each curve is $T = 3000$ s and the time bin of the SPCM is set to $\Delta t_{\rm bin} = 1$ ns. The repetition rate of the measurement is 100 Hz. The joint-detection efficiency of our system is $\eta = \eta_{\rm c}\eta_{\rm F1}\eta_{\rm F2}\eta_{\rm D}^2 \approx 4\%$, where $\eta_{\rm c}$ is the Stokes to anti-Stokes coupling efficiency, $\eta_{\rm F1}$ and $\eta_{\rm F2}$ are the transmission efficiency of the narrow band filters, and $\eta_{\rm D}$ is the detection efficiency of the SPCM. With a duty cycle $\xi = 5\%$, the coincidence counts can be calculated from the formula $\mathrm{CCount}(\tau) = \eta\xi|\psi(\tau)|^2\Delta t_{\rm bin}T$. We first set $z_0 = -0.5$ mm and $\Delta z' = 0$, which correspond to a pump-beam profile shown in Fig. 2(a1), and obtain a Gaussian-shape single photon waveform shown in Fig. 2(a2). After that, we adjust the LTS to set $\Delta z' = -0.3$ mm and $\Delta z' = 0.3$ mm and obtain the waveforms shown in Figs. 2(b2) and 2(c2), which correspond to the profiles in Figs. 2(b1) and 2(c1), respectively. These results demonstrate that by adjusting the LTS to shift the profile of the pump beam along the 2D MOT, the peak position of the Gaussian-shape waveforms of the heralded single photons can be well controlled. The pairing rates of the Stokes and anti-Stokes photons from the atomic ensemble are calculated to be about 14000, 11000 and 8000 pair/s for Figs. 2(a2), 2(b2) and 2(c2), respectively, while the corresponding heralded efficiencies are about 0.36, 0.36 and 0.31.

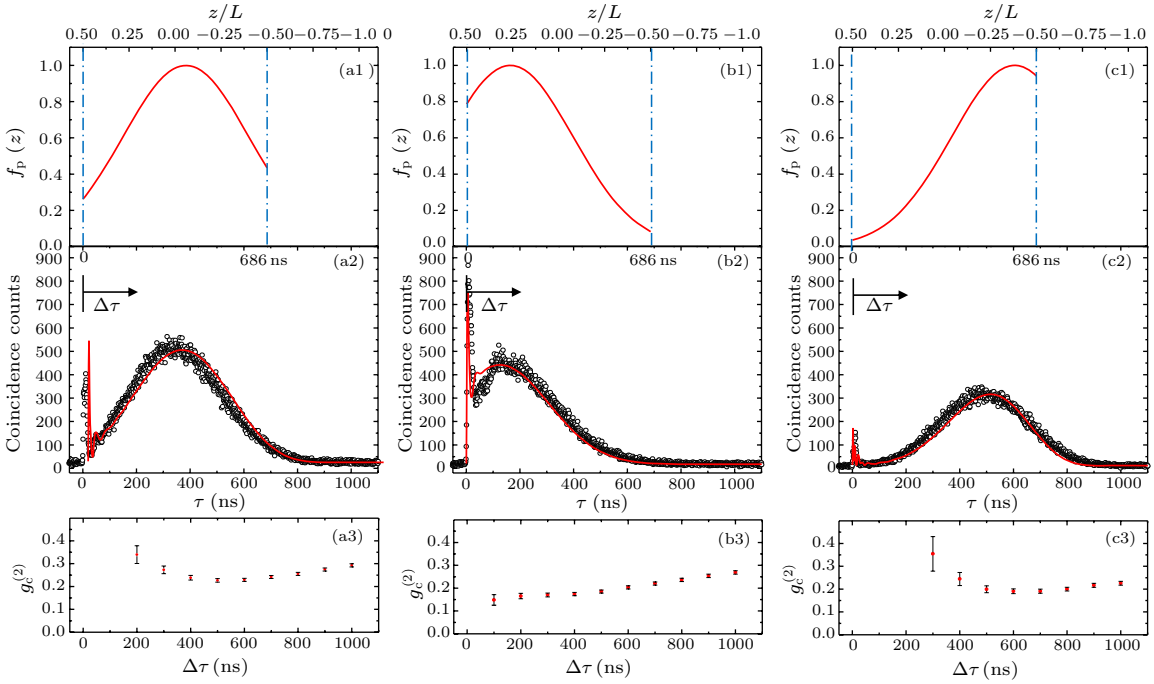

Fig. 2. The Gaussian-shape waveforms of the heralded single photons. Here (a1), (b1) and (c1) are the profiles of the pump beam along the z axis ($z = 0$ is the center of the MOT); (a2), (b2) and (c2) are the corresponding coincidence counts of the measured heralded single photons in 3000 s; (a3), (b3) and (c3) are the corresponding $g_{\rm c}^{(2)}$ of the measured heralded single photons.

In addition to the waveform, we also investigate the non-classical nature of the single anti-Stokes photons with a Hanbury–Brown–Twiss (HBT) interferometer,[41] which shows the non-separability of a single photon. By sending the anti-Stokes photon to a 50/50 fiber beam splitter (FBS), we obtain its con-

ditional zero delay 2nd order auto-correlation function $g_c^{(2)} = N_G N_{GTR}/(N_{GT} N_{GR})$, where N_G is the Stokes photon counts, N_{GR} (N_{GT}) is the twofold coincidence counts between the Stokes photon and the anti-Stokes photon coming out of the reflection (transmission) port of FBS, and N_{GTR} is the threefold coincidence counts between the Stokes photon and the anti-Stokes photon coming out of both ports of FBS. Here a pure single photon state promises $g_c^{(2)} = 0$, while a two-photon state gives $g_c^{(2)} = 0.5$. The measured 2nd order auto-correlation function of the heralded single photon is shown in Figs. 2(a3), 2(b3) and 2(c3). It shows that in all the three cases, $g_c^{(2)} < 0.5$ holds well within the entire temporal waveform and indicates a good single-photon nature.

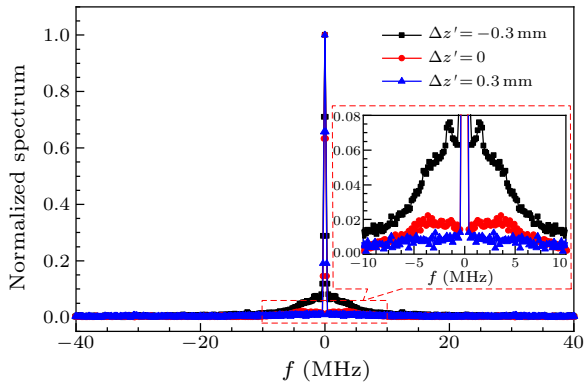

Fig. 3. The normalized spectrum of the heralded single photon's temporal waveform. The black squares, red circles and blue triangles correspond to $\Delta z' = -0.3$ mm, $\Delta z' = 0$ and $\Delta z' = +0.3$ mm, respectively.

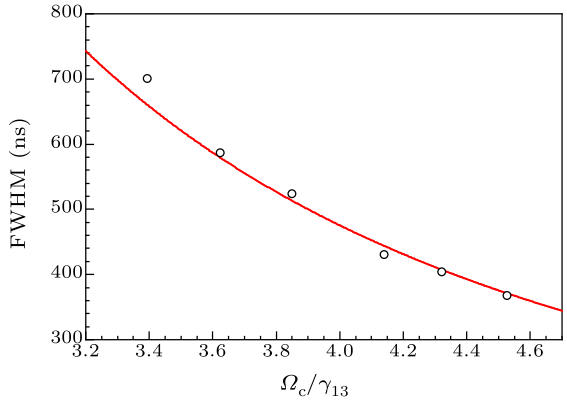

Fig. 4. The full width at half maximum (FWHM) of the Gaussian-shape heralded single photon versus different Rabi frequencies of the coupling beam (Ω_c). The red solid curve is the theoretical curve and the black squares are the experimental data. Here γ_{13} is the decay rate between $|1\rangle$ and $|3\rangle$.

Furthermore, we analyze the spectrum of the heralded single photon's temporal waveform in Fig. 3. The spectra contain different sidebands while have the same centreband. For the EIT-based quantum memory, which is a promising way in achieving the high efficiency single photon storage, the storage bandwidth is usually several MHz.[15–17,42] Thus the sidebands in the heralded single photon's spectrum will lead to the decrease of both the storage efficiency and the fidelity. The sidebands are mainly caused by the sharp spike in front of the main Gaussian-shape waveform, which is called the optical precursor.[43] We also find in Fig. 3 that as $\Delta z'$ increases, the sidebands are suppressed. As shown in Figs. 2(a2), 2(b2) and 2(c2), as the main Gaussian-shape waveform moves away from the precursor, the coincidence counts of the optical precursor decrease faster than the coincidence counts of the main Gaussian-shape waveform. However, if the main Gaussian-shape waveform keeps moving away from the precursor, the signal-to-noise ratio will get worse and worse as the total signal decreases and finally leads to the destruction of the single-photon nature. Hence, in the practical application for the quantum storage, both the sideband and the single-photon nature should be considered simultaneously to obtain an optimal waveform.

In the following we show how to control the FWHM of the heralded single photon's temporal waveform by adjusting the Rabi frequency of the coupling beam. The OD here is about 126. The pump-beam Rabi frequency is kept to be stable and $\Delta z' = 0$ is also maintained during the experiment. The FWHM is proportional to $|\psi(\tau)|^2$. Considering Eqs. (1) and (3), we could obtain $\text{FWHM} = \frac{\sqrt{2\ln 2} w_0}{V_g \sin\theta} = \frac{(2\sqrt{2\ln 2})\text{OD} w_0 \gamma_{13}}{\Omega_c^2 L \sin\theta}$. As shown in Fig. 4, the experimental data fit the theoretical curve very well. By controlling the FWHM of the temporal waveform, the bandwidth of the Gaussian-shape single photons can be modified to meet the requirement of the EIT-based quantum memory.[15,16]

In conclusion, we have generated Gaussian-shape narrowband heralded single photons with a simple and self-stabilizing spatial light modulation technique. By adjusting the Rabi frequency of the coupling beam and the LTS, both the FWHM and the peak position of the Gaussian-shape waveform can be controlled. The HBT measurement shows that the condition $g_c^{(2)} < 0.5$ holds well within the entire temporal waveform, which indicates a very good single-photon nature. Furthermore, we have also found that the sidebands of the heralded single photons in frequency domain can be suppressed by adjusting the peak position of the waveform. With this source, we have achieved a $> 90\%$ efficiency quantum storage and the result is shown in Ref. [44]. We believe that this source will have a potential application in quantum information processing.

References

[1] Jacques V, Wu E, Grosshans F, Treussart F, Grangier P,

Aspect A and Roch J 2007 *Science* **315** 966
[2] Tang J S, Li Y L, Xu X Y, Xiang G Y, Li C F and Guo G C 2012 *Nat. Photon.* **6** 600
[3] Yan H, Liao K Y, Deng Z T, He J Y, Xue Z Y, Zhang Z M and Zhu S L 2015 *Phys. Rev. A* **91** 042132
[4] Kolobov M I 1999 *Rev. Mod. Phys.* **71** 1539
[5] Gisin N, Ribordy G, Tittel W and Zbinden H 2002 *Rev. Mod. Phys.* **74** 145
[6] Galindo A and Martín-Delgado M A 2002 *Rev. Mod. Phys.* **74** 347
[7] Nicolas S, Christoph S, Hugues de R and Nicolas G 2011 *Rev. Mod. Phys.* **83** 33
[8] Kwiat P G, Mattle K, Weinfurter H, Zeilinger A, Sergienko A V and Shih Y H 1995 *Phys. Rev. Lett.* **75** 4337
[9] Wang F Y, Shi B S and Guo G C 2008 *Opt. Lett.* **33** 2191
[10] Bao X H, Qian Y, Yang J, Zhang H, Chen Z B, Yang T and Pan J W 2008 *Phys. Rev. Lett.* **101** 190501
[11] Duan L M, Lukin M D, Cirac J I and Zoller P 2001 *Nature* **414** 413
[12] Hedges M P, Longdell J J, Li Y and Sellars M J 2010 *Nature* **465** 1052
[13] Cho Y W, Campbell G T, Everett J L, Bernu J, Higginbottom D B, Cao M T, Geng J, Robins N P, Lam P K and Buchler B C 2016 *Optica* **3** 100
[14] Reim K F, Michelberger P, Lee K C, Nunn J, Langford N K and Walmsley I A 2011 *Phys. Rev. Lett.* **107** 053603
[15] Chen Y H, Lee M J, Wang I C, Du S W, Chen Y F, Chen Y C and Yu I A 2013 *Phys. Rev. Lett.* **110** 083601
[16] Hsiao Y F, Tsai P J, Chen H S, Lin S X, Hung C C, Lee C H, Chen Y H, Chen Y F, Yu Ite A and Chen Y C 2018 *Phys. Rev. Lett.* **120** 183602
[17] Vernaz-Gris P, Huang K, Cao M, Alexandra S S and Julien L 2018 *Nat. Commun.* **9** 363
[18] Balic V, Braje D A, Kolchin P, Yin G Y and Harris S E 2005 *Phys. Rev. Lett.* **94** 183601
[19] Kolchin P, Du S W, Belthangady C, Yin G Y and Harris S E 2006 *Phys. Rev. Lett.* **97** 113602
[20] Yan H, Zhang S C, Chen J F, Loy M M T, Wong G K L and Du S W 2011 *Phys. Rev. Lett.* **106** 033601
[21] Shu C, Chen P, Chow T K A, Zhu L B, Xiao Y H, Loy M M T and Du S W 2016 *Nat. Commun.* **7** 12783
[22] Srivathsan B, Gulati G K, Chng B, Maslennikov G, Matsukevich D and Kurtsiefer C 2013 *Phys. Rev. Lett.* **111** 123602
[23] Liao K Y, Yan H, He J Y, Du S W, Zhang Z M and Zhu S L 2014 *Phys. Rev. Lett.* **112** 243602
[24] Liao K Y, Yan H, He J Y, Huang W, Zhang Z M and Zhu S L 2014 *Chin. Phys. Lett.* **31** 034205
[25] Farrera P, Heinze G, Albrecht B, Ho M, Chavez M, Teo C, Sangouard N and de Riedmatten H 2016 *Nat. Commun.* **7** 13556
[26] Chen Q F, Shi B S, Feng M, Zhang Y S and Guo G C 2008 *Opt. Express* **16** 21708
[27] Lu X S, Chen Q F, Shi B S and Guo G C 2009 *Chin. Phys. Lett.* **26** 064204
[28] Chen P, Zhou S Y, Xu Z, Duan Y F, Cui G D, Hong T and Wang Y Z 2011 *Chin. Phys. Lett.* **28** 074214
[29] Han Z G, Qian P, Zhou L, Chen J F and Zhang W P 2015 *Sci. Rep.* **5** 9126
[30] Park K K, Kim J H, Zhao T M, Cho Y W and Kim Y H 2017 *Optica* **4** 1293
[31] Novikova I, Gorshkov A V, Phillips D F, Sorensen A S, Lukin M D and Walsworth R L 2007 *Phys. Rev. Lett.* **98** 243602
[32] Wang Y M, Minář J, Sheridan L and Scarani V 2011 *Phys. Rev. A* **83** 063842
[33] Liu C, Sun Y, Zhao L W, Zhang S C, Loy M M T and Du S W 2014 *Phys. Rev. Lett.* **113** 133601
[34] Kolchin P, Belthangady C, Du S W, Yin G Y and Harris S E 2008 *Phys. Rev. Lett.* **101** 103601
[35] Chen J F, Zhang S C, Yan H, Loy M M T, Wong G K L and Du S W 2010 *Phys. Rev. Lett.* **104** 183604
[36] Zhao L, Guo X, Sun Y, Su Y, Loy M M T and Du S W 2015 *Phys. Rev. Lett.* **115** 193601
[37] Zhao L W, Su Y M and Du S W 2016 *Phys. Rev. A* **93** 033815
[38] Ketterle W, Davis K B, Joffe M A, Martin A and Pritchard D E 1993 *Phys. Rev. Lett.* **70** 2253
[39] Lin Y W, Chou H C, Dwivedi P P, Chen Y C and Yu I A 2008 *Opt. Express* **16** 3753
[40] Zhang S, Chen J F, Liu C, Zhou S, Loy M M T, Wong G K L and Du S W 2012 *Rev. Sci. Instrum.* **83** 073102
[41] Grangier P, Roger G and Aspect A 1986 *Europhys. Lett.* **1** 173
[42] Zhang S C, Zhou S Y, Loy M M T, Wong G K L and Du S W 2011 *Opt. Lett.* **36** 4530
[43] Chen J F, Jeong H, Feng L, Loy M M T, Wong G K L and Du S W 2010 *Phys. Rev. Lett.* **104** 223602
[44] Wang Y F, Li J F, Zhang S C, Su K Y, Zhou Y R, Liao K Y, Du S W, Yan H and Zhu S L 2019 *Nat. Photon.* **13** 346